J Incl Phenom Macrocycl Chem (2009) 65:269–286
DOI 10.1007/s10847-009-9578-x

ORIGINAL ARTICLE

Phosphorus–nitrogen compounds: part 16. Synthesis, stereogenism, anisochronism and the relationship between ^{31}P NMR spectral and crystallographic data of monotopic *spiro*-crypta phosphazene derivatives

Zeynel Kılıç · Aytuğ Okumuş · Şemsay Demiriz · Selen Bilge · Aslı Öztürk · Nagihan Çaylak · Tuncer Hökelek

Received: 30 January 2009 / Accepted: 25 March 2009 / Published online: 8 April 2009

Abstract The condensation reactions of N_2O_3-donor type coronands (**1**–**3**) with hexachlorocyclotriphosphazatriene, $N_3P_3Cl_6$, resulted in the formation of *spiro*-crypta phosphazene derivatives (**4**–**6**). These compounds with excess morpholine and 1,4-dioxa-8-azaspiro[4,5]decane (DASD) afford fully substituted morpholino (**7** and **10**) and 1,4-dioxa-8-azaspiro[4,5]deca (**8**)-substituted phosphazene derivatives, respectively. Whilst, in the same conditions, the reactions of **4**, **5** and **6** with pyrrolidine, morpholine and DASD also produce partially pyrrolidino-substituted geminal (**9** and **11**), mono-substituted pyrrolidino (**12**), morpholino (**13**) and 1,4-dioxa-8-azaspiro[4,5]deca (**14**) phosphazenes. It has been clearly observed that the chloride replacement reactions of **4**, **5** and **6** with pyrrolidine lead to the geminal products. Compounds **7**, **8** and **10** are the first examples of anisochronic tetrakis (amino) phosphazenes according to ^{31}P NMR data. The structures of **7**, **8** and **10**–**14** have been determined by FTIR, MS, ^{1}H, ^{13}C and ^{31}P NMR, DEPT, and HETCOR spectral data. The solid-state structures of **9**, **13** and **14** have been examined by X-ray diffraction techniques. The sums of the bond angles around the *spiro* cyclic nitrogen atoms [344.8(4)° and 347.6(4)°] of **9**, indicate that the nitrogen atoms have pyramidal geometries. Thus, the N atoms seem to have stereogenic configurations. Compounds **12**–**14** also have two stereogenic P-atoms, and they are expected to be in the mixture of enantiomers. The relationships between NPN (α and α') bond angles and δP_{spiro} values and the correlation of Δ(P–N) with δP_{spiro} and $\Delta(\delta P)$ values are presented.

Keywords *Spiro*-crypta-phosphazenes · Anisochronism · Stereogenism · Spectroscopy · X-ray crystallography

Z. Kılıç (✉) · A. Okumuş · Ş. Demiriz · S. Bilge
Department of Chemistry, Ankara University, 06100 Tandogan, Ankara, Turkey
e-mail: zkilic@science.ankara.edu.tr

A. Öztürk · T. Hökelek
Department of Physics, Hacettepe University, 06800 Beytepe, Ankara, Turkey

N. Çaylak
Department of Physics, Sakarya University, 54187 Esentepe, Adapazarı, Turkey

Introduction

The word phosphazene refers to a broad range of molecules, all of which contain phosphorus and nitrogen atoms joined by formally unsaturated bonds. These units can be linked together to form either chains or rings. The hexachlorocyclotriphosphazene, $N_3P_3Cl_6$, is the best known and the most intensively studied in the field of phosphazene chemistry. Most of the phosphazene compounds have been prepared by nucleophilic substitution reactions on $N_3P_3Cl_6$ due to the ease of introducing a wide variety of organic, inorganic and organometallic substituents onto P-centres [1]. Additionally, *cyclo*-phosphazenes can be used as building blocks for macromolecular and polymeric species [2]. The ring-opening-polymerization (ROP) of $N_3P_3Cl_6$ leads to the preparation of different polyphosphazene types; cyclolinear or cyclomatrix polymers [3, 4]. They continue to attract the increased attention of researchers in recent years, since they are candidates to be used in alternative industrial applications in areas such as high performance elastomers [5], rechargeable lithium batteries and polymer electrolytes [6, 7], biomedical materials including synthetic bones [8], and biomedical membranes [9]. The syntheses and the characterizations of

chiral phosphazene bases have also been an area of interest [10–12]. Recently, our group has focused on the replacement reactions of Cl atoms of $N_3P_3Cl_6$ by bulky nucleophiles such as; aromatic diamines [13–15], N_xO_y-donor type (x,y = 2–4) dibenzo-diaza-crown ethers (coronands) [16–23], diaminophenolates [24–26], and diphenolates [27–29] to obtain novel phosphazene derivatives with different architectures, namely *spiro*-, *ansa*-, di*spiro*-, tri*spiro*-, *spiro-ansa*-, *spiro-ansa-spiro*-, *spiro-bino-spiro*- and *spiro*-crypta-skeletons.

The present work reports (1) the substitutions of Cl atoms of $N_3P_3Cl_4\{Ph_2[O(CH_2CH_2O)][CH_2N(CH_2)_n NCH_2]\}$ [n = 2 (**4**) [17, 18], n = 3 (**5**) [17], n = 4 (**6**) [19]] by pyrrolidine, morpholine and DASD that give partially pyrrolidine-substituted geminal $N_3P_3Cl_2(C_4H_8N)_2\{Ph_2[O(CH_2CH_2O)][CH_2N(CH_2)_nNCH_2]\}$ [n = 3 (**9**), n = 4 (**11**)], fully morpholine-substituted $N_3P_3(C_4H_8NO)_4\{Ph_2[O(CH_2CH_2O)][CH_2N(CH_2)_nNCH_2]\}$ [n = 2 (**7**), n = 3 (**10**)], fully DASD substituted $N_3P_3(C_7H_{12}NO_2)_4\{Ph_2[O(CH_2CH_2O)][CH_2N(CH_2)_nNCH_2]\}$ [n = 2 (**8**)], and mono pyrrolidine, morpholine and DASD substituted $N_3P_3Cl_5Z\{Ph_2[O(CH_2CH_2O)][CH_2N(CH_2)_4NCH_2]\}$ [Z = C_4H_8N (**12**), Z = C_4H_8NO (**13**), Z = $C_7H_{12}NO_2$ (**14**), respectively] phosphazene derivatives (Scheme 1); (2) the structures of all the compounds determined by elemental analyses, MS, IR, ^1H, ^{13}C and ^{31}P NMR, DEPT and HETCOR spectral data; (3) the X-ray structural analyses of **9**, **13** and **14**; and (4) the relationship between the δP_{spiro}-shifts and the endocyclic (α) and exocyclic (α') NPN bond angles, and the relationship between Δ(P–N) values and $\Delta(\delta P)$ chemical shift differences as well as δP_{spiro}-shifts.

Experimental

General methods

All reactions were carried out under argon atmosphere. The reaction solvents were dried and purified by standard

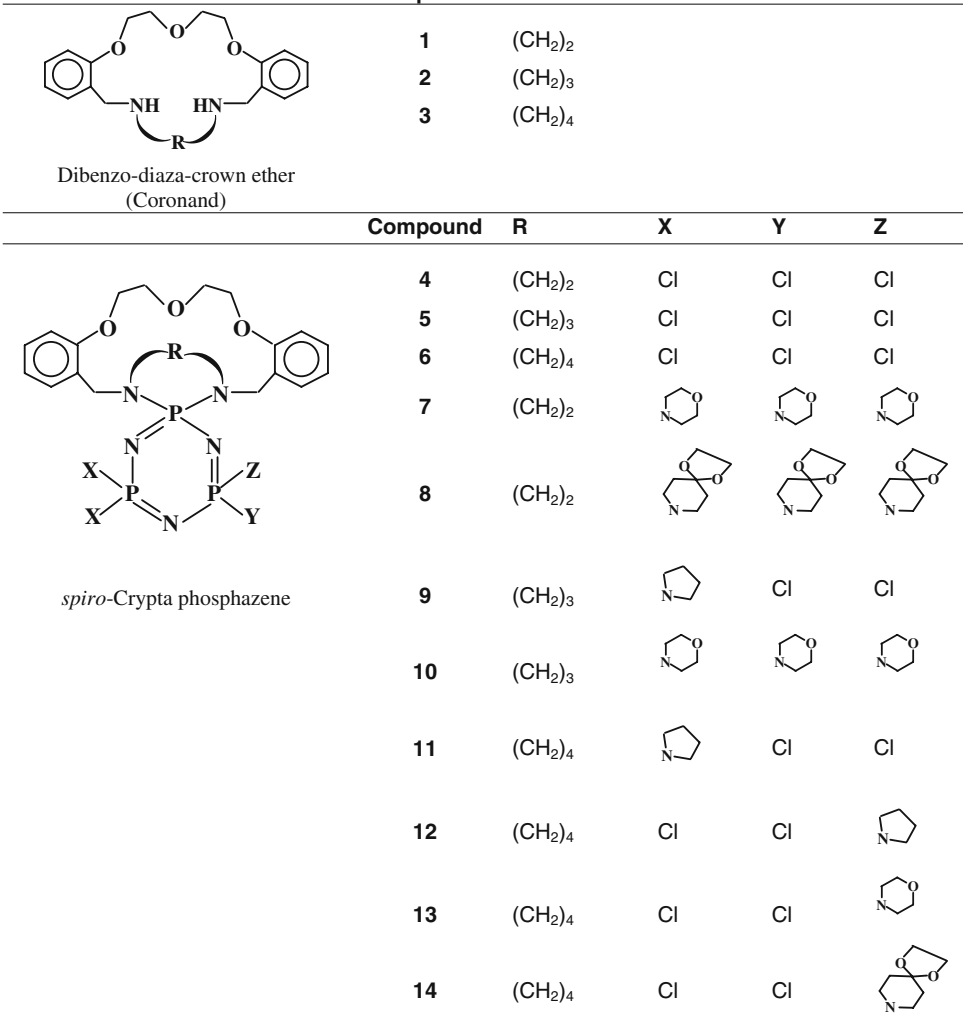

Scheme 1 The formulae of monotopic-*spiro*-crypta phosphazene derivatives

methods [30]. Melting points were measured on a Gallenkamp apparatus using a capillary tube. ^{1}H, ^{13}C, ^{31}P NMR and HETCOR spectra were obtained on a Bruker DPX FT-NMR (400 MHz) spectrometer ($SiMe_4$ as internal and 85% H_3PO_4 as external standards). IR spectra were recorded on a Mattson 1000 FTIR spectrometer in KBr discs and reported in cm^{-1} units. Microanalyses were carried out by the microanalytical service of TÜBİTAK-Turkey. API-ES mass spectrometric analyses were performed on the AGILEND 1100 MSD spectrometer. Thin-layer chromatography (TLC) was performed on Merck DC Alufolien Kiesegel 60 B_{254} sheets. Column chromatography was performed on Merck Kiesegel 60 (230–400 mesch ATSM) silica gel.

Preparation of compounds

Dibenzo-diaza-crown ethers (**1**–**3**) [19, 31, 32] and phosphazene derivatives **4**–**6** and **9** were prepared according to the published procedures [17–19]. The preparation and MS, IR, ^{1}H, ^{13}C and ^{31}P NMR data of **9** were published before [19] but, the crystallographic data of **9** will be discussed herein.

Synthesis of 7,10-(Pentane-3-oxa-1,5-diyldioxydi-o-phenylene-dimethylene)-4,4,6,6-tetrakis(morpholino-1-yl)-2λ^5,4λ^5,6λ^5-triphosphaza(6-P^V)-1,3,5,7,10-pentaazaspiro[4.5]undeca-1,3,5-triene(**7**): A solution of morpholine (0.68 g, 7.91 mmol) in 50 mL of THF was slowly added to a stirred solution of **4** (0.40 g, 0.65 mmol) in 100 mL of dry THF at ambient temperature. The solution was heated to reflux for 36 h with argon being passed over the reaction mixture. The precipitated morpholine hydrochloride was filtered off, and the solvent was evaporated at reduced pressure. The residue was subjected to column chromatography [benzene/THF (3:1)] and crystallized from CH_3CN (yield: 0.35 g, 66%, m.p. 244 °C). Anal. Cald. for $C_{36}H_{56}N_9O_7P_3 \cdot H_2O$: C, 51.69%; H, 5.98%; N, 14.76%. Found C, 51.61%; H, 6.98%; N, 15.05%. IR (KBr, cm^{-1}, selected peaks): 3456 *v* (OH), 3065 *v* (aromatic CH asymm.), 3025 *v* (aromatic CH symm.), 1599 *v* (C=C), 1196 *v* (P=N). MS (API) (Ir %): m/z = 820 [$(MH)^+$, 100%].

Synthesis of 7,10-(Pentane-3-oxa-1,5-diyldioxydi-o-phenylene-dimethylene)-4,4,6,6-tetrakis(1,4-dioxa-8-azaspiro[4,5] decane-1-yl)-2λ^5,4λ^5,6λ^5-triphosphaza(6-P^V)-1,3,5,7,10-pentaazaspiro[4.5]undeca-1,3,5-triene (**8**): The work-up procedure as compound **7**, using **4** (0.60 g, 0.97 mmol), and DASD (1.67 g, 11.7 mmol) (36 h). The product was purified by column chromatography by using [benzene/THF (1:1)] and crystallized from n-heptane (yield: 0.61 g, 61%, m.p. 276 °C). Anal Cald. for $C_{48}H_{72}N_9O_{11}P_3$: C, 55.89%; H, 5.20%; N, 11.96%. Found C, 55.22%; H, 6.95%; N, 12.07%. IR (KBr, cm^{-1}, selected peaks): 3065 *v* (aromatic CH asymm.), 3025 *v* (aromatic CH symm.), 1597 *v* (C=C), 1186 *v* (P=N). MS (API) (Ir %): m/z = 901 [$(M\text{-}DASD)^+$, 0.4%], m/z = 760 [$(MH\text{-}2\ DASD)^+$, 0.9%].

Synthesis of 7,11-(Pentane-3-oxa-1,5-diyldioxydi-o-phenylene-dimethylene)-4,4,6,6-tetrakis(morpholino-1-yl)-2λ^5,4λ^5,6λ^5-triphosphaza(6-P^V)-1,3,5,7,11-pentaazaspiro[5.5]dodeca-1,3,5-triene (**10**): A solution of morpholine (2.00 g, 23.3 mmol) in 50 mL of THF was slowly added to a stirred solution of **5** (1.20 g, 1.90 mmol) in 100 mL of dry THF at room temperature. The solution was heated to reflux for 40 h with argon being passed over the mixture. The precipitated morpholine hydrochloride was filtered off, and the solvent was evaporated at reduced pressure. The residue was subjected to column chromatography [benzene/THF (3:1)] and the product crystallized from [n-heptane/THF (1:1)] (yield: 1.10 g, 70%, m.p. 177 °C). Anal Cald for $C_{37}H_{58}N_9O_7P_3$: C, 52.91%; H, 6.98%; N, 14.57%. Found C, 53.3%; H, 7.01%; N, 15.12%. IR (KBr, cm^{-1}, selected peaks): 3070 *v* (aromatic CH asymm.), 3025 *v* (aromatic CH symm.), 1597 *v* (C=C), 1192 *v* (P=N). MS (API) (Ir %): m/z = 834 [$(MH)^+$, 100%].

Syntheses of 7,12-(Pentane-3-oxa-1,5-diyldioxydi-o-phenylene-dimethylene)-4,4-dichloro-6,6-bis(pyrrolidino-1-yl)-2λ^5,4λ^5,6λ^5-triphosphaza(6-P^V)-1,3,5,7,12-pentaazaspiro[6.5]trideca-1,3,5-triene (**11**) *and 7,12-(Pentane-3-oxa-1,5-diyldioxydi-o-phenylene-dimethylene)-4,4,6-trichloro-6-mono (pyrrolidino-1-yl)-2λ^5,4λ^5,6λ^5-triphosphaza(6-P^V)-1,3,5,7,12-pentaazaspiro [6.5]trideca-1,3,5-triene* (**12**): A solution of pyrrolidine (1.50 g, 20 mmol) in 50 mL of THF was slowly added to a stirred solution of **6** (1.10 g, 1.7 mmol) in 100 mL of dry THF at ambient temperature. The solution was heated to reflux for 48 h with argon being passed over the mixture. The precipitated pyrrolidine hydrochloride was filtered off, and the solvent was evaporated at reduced pressure. The residue was subjected to column chromatography [benzene/THF (4:1)]. Compounds **11** and **12** were crystallized from benzene and *n*-heptane/THF (1:1) respectively. Data of **11**: (yield: 0.60 g, 49%, m.p. 190 °C). Anal Cald for $C_{30}H_{44}N_7O_3P_3Cl_2$: C, 50.60%; H, 6.23%; N, 13.54%. Found C, 50.43%; H, 6.21%; N, 13.72%. IR (KBr, cm^{-1}, selected peaks): 3066 *v* (aromatic CH asymm.), 3021 *v* (aromatic CH symm.), 1599 *v* (C=C), 1182 *v* (P=N), 556, 488 *v* (P–Cl). MS (API) (fragments based on ^{35}Cl, Ir %): m/z = 714 [$(MH)^+$, 100%]. Data of **12**: (yield: 0.30 g, 26%, m.p. 176 °C). Anal Cald for $C_{26}H_{36}N_6O_3P_3Cl_3 \cdot C_6H_6$: C, 49.36%; H, 6.02%; N, 11.09%. Found C, 50.66%; H, 5.54%; N, 11.08%. IR (KBr, cm^{-1}, selected peaks): 3064 *v* (aromatic CH asymm.), 3022 *v* (aromatic CH symm.), 1599 *v* (C=C), 1184, 1234 *v* (P=N), 558, 482 *v* (P–Cl). MS (API) (fragments based on ^{35}Cl, Ir %): m/z = 679 [$(MH)^+$, 100%].

Synthesis of 7,12-(Pentane-3-oxa-1,5-diyldioxydi-o-phenylene-dimethylene)-4,4,6-trichloro-6-mono(morpholino-1-yl)-2λ^5,4λ^5,6λ^5-triphosphaza(6-P^V)-1,3,5,7,12-pentaazaspiro

[6.5]trideca-1,3,5-triene (**13**): A solution of morpholine (0.80 g, 9.30 mmol) in 50 mL of THF was slowly added to a stirred solution of **6** (0.50 g, 0.78 mmol) in 100 mL of dry THF at room temperature. The solution was heated to reflux for 48 h with argon being passed over the mixture. The precipitated morpholine hydrochloride was filtered off, and the solvent was evaporated at reduced pressure. The residue was subjected to column chromatography [benzene/THF (3:1)] and the product (**13**) was crystallized from [*n*-heptane/THF (1:1)] (yield: 0.38 g, 70%, m.p. 193 °C). Anal Cald for $C_{26}H_{36}N_6O_4P_3Cl_3$: C, 45.67%; H, 5.16%; N, 11.35%. Found C, 44.88%; H, 5.21%; N, 12.08%. IR (KBr, cm^{-1}, selected peaks): 3065 *v* (aromatic CH asymm.), 3034 *v* (aromatic CH symm.), 1595 *v* (C=C), 1182, 1229 *v* (P=N), 554, 483 *v* (P–Cl). MS (API) (fragments based on ^{35}Cl, Ir %): m/z = 695 [(M*H*)$^+$, 100%].

Synthesis of 7,12-(Pentane-3-oxa-1,5-diyldioxydi-o-phenylene-dimethylene)-4,4,6-trichloro-6-mono(1,4-dioxa-8-azaspiro [4,5]decane-1-yl)-2λ^5,4λ^5,6λ^5-triphosphaza (6-P^V)-1,3,5,7,12-pentaazaspiro[6.5]trideca-1,3,5-triene (**14**): The work-up procedure as compound **13**, using **6** (0.60 g, 0.93 mmol), and DASD (1.60 g, 11.2 mmol) (48 h). The product was purified by column chromatography by using [benzene/THF (2:1)] and crystallized from CH_3CN (yield: 0.46 g, 67%, m.p. 186 °C). Anal Cald for $C_{29}H_{40}N_6O_5P_3Cl_3 \cdot CH_3CN$: C, 46.42%; H, 5.43%; N, 11.72%. Found C, 46.14%; H, 5.55%; N, 12.55%. IR (KBr,cm^{-1}, selected peaks): 3067 *v* (aromatic CH asymm.), 3033 *v* (aromatic CH symm.), 1597 *v* (C=C), 1181, 1231 *v* (P=N), 552, 485 *v* (P–Cl). MS (API) (fragments based on ^{35}Cl, Ir %): m/z = 750 [M$^+$, 24%].

X-Ray crystallography

Colourless crystals of **9** and **14** were grown from CH_3CN, while **13** was grown from *n*-heptane/THF (1:1) at room temperature. The molecular structures and the packing diagrams of compounds (**9**, **13** and **14**) along with the atom-numbering schemes are depicted in Figs. 1, 2 and 3. Crystallographic data are listed in Table 1 and selected bond lengths and angles are given in Table 2. Crystallographic data were collected on an Enraf-Nonius (for **9** and **14**) and Bruker Kappa APEXII (for **13**) diffractometers using Cu K_α radiation (λ = 1.54184 Å) (for **9**) and Mo K_α radiation (λ = 0.71073 Å) (for **13** and **14**) at T = 294 K. Absorption corrections by psi-scan [33] (for **9** and **14**) and

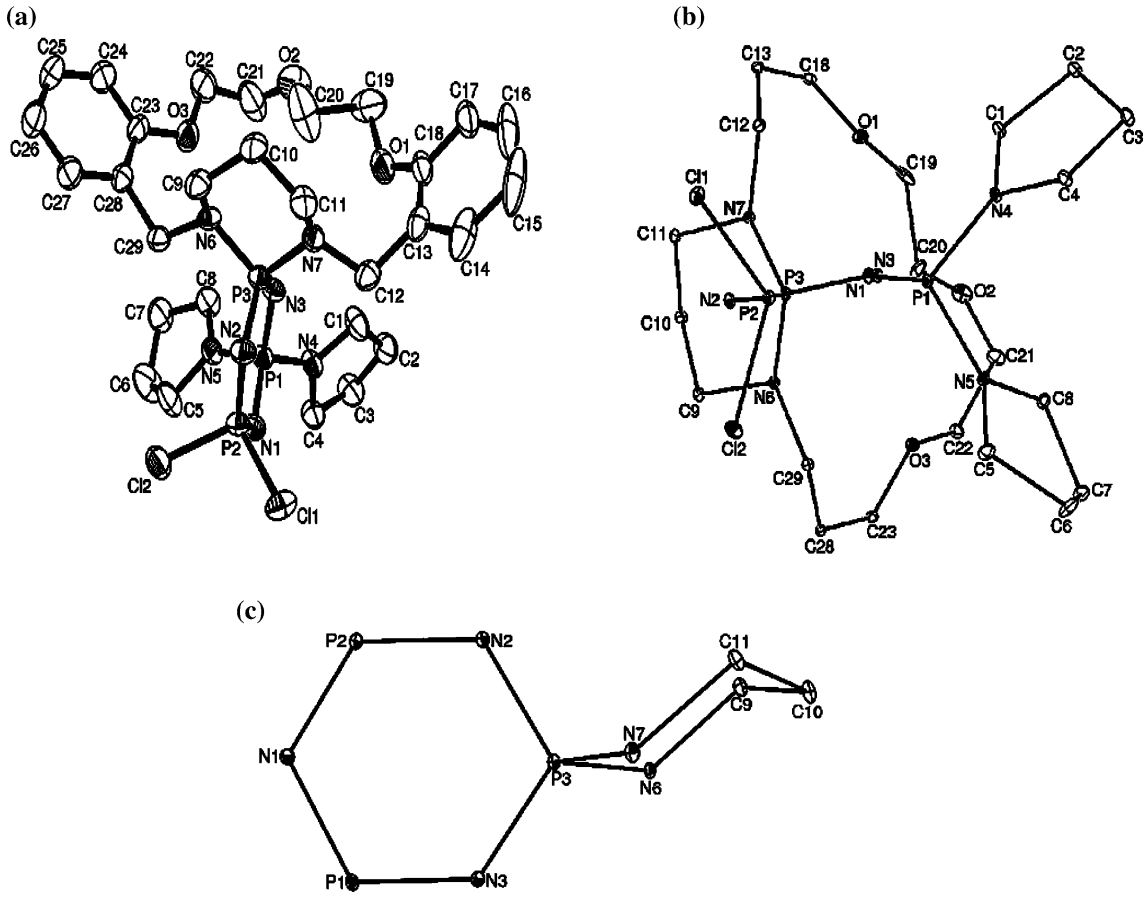

Fig. 1 **a** An ORTEP-3 [36] drawing of **9** with the atom-numbering scheme. Displacement ellipsoids are drawn at the 30% probability level. **b** The conformations of the phosphazene and the macrorings. **c** The conformation of the six-membered *spiro*-ring

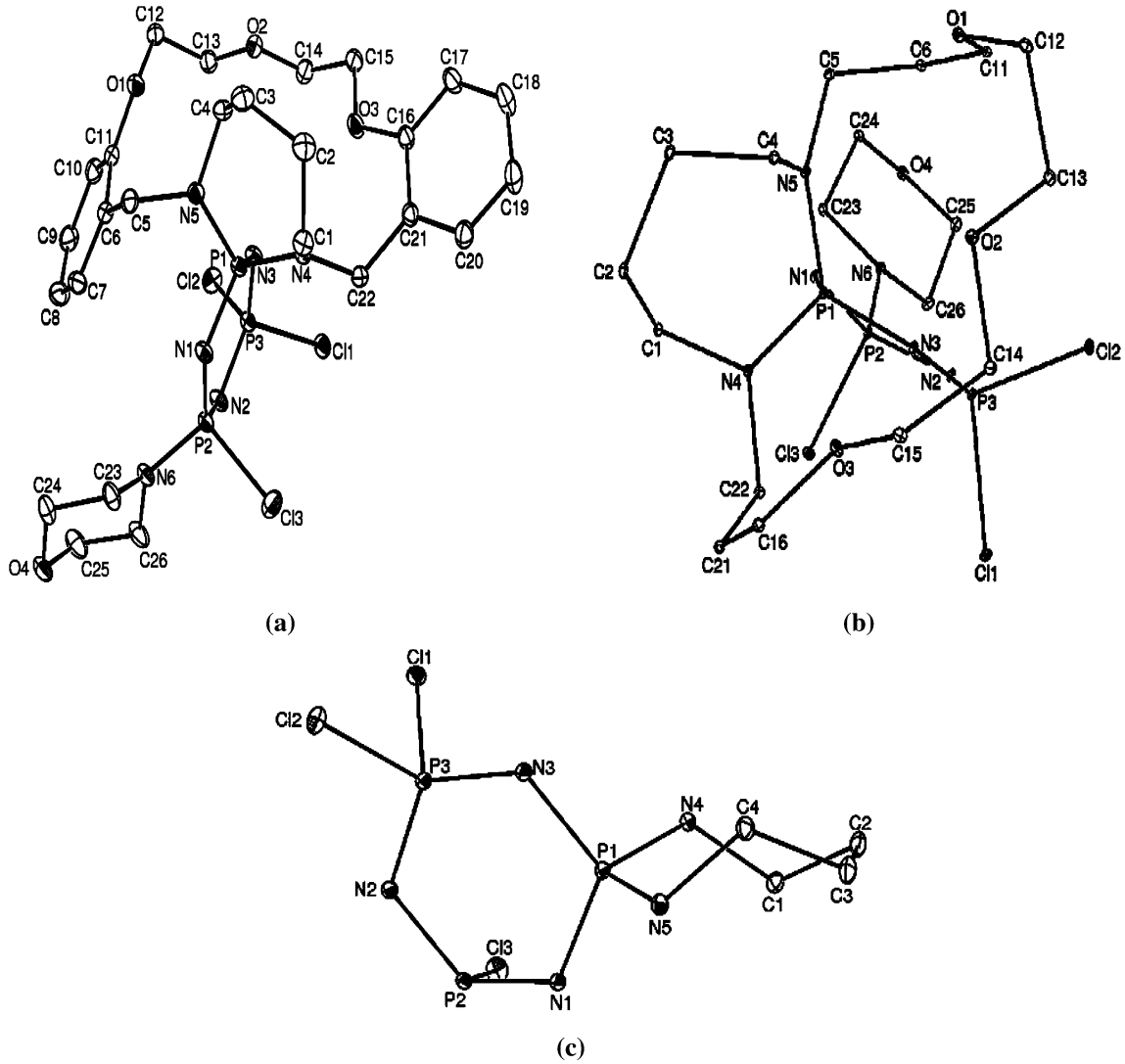

Fig. 2 **a** An ORTEP-3 [36] drawing of **13** with the atom-numbering scheme. Displacement ellipsoids are drawn at the 30% probability level. **b** The conformations of the phosphazene and the macrorings. **c** The conformation of the seven-membered *spiro*-ring

multi-scan [34] (for **13**) were applied. Structures were solved by direct methods [35] and refined by full-matrix least squares against F^2 using all data [35]. All non-H atoms were refined anisotropically. The H atom positions were calculated geometrically at distances of 0.93 (CH), 0.97 Å (CH_2) and 0.96 Å (CH_3) from the parent C atoms; a riding model was used during the refinement process and the U_{iso}(H) values were constrained to be $1.2U_{eq}$(carrier atom).

Results and discussion

Synthesis

The new phosphazene derivatives (**7**, **8** and **10–14**; Scheme 1) are obtained from the reactions of monotopic crypta phosphazenes **4**, **5** and **6** with pyrrolidine, morpholine and DASD in THF. Crypta phosphazenes are the tricyclic compounds, made up of diaza-crown ethers (coronands) and phosphazene rings [19]. Scheme 2 shows the chloride replacement reactions, [dominantly SN^1(P)], of crypta phosphazenes with secondary amines. The condensation reactions of crypta phosphazenes with excess pyrrolidine, morpholine and DASD produce three kinds of compounds; e.g. mono substituted N_3P_3(diazacrown)(amine)Cl_3 [amine; pyrrolidine (**12**), morpholine (**13**), and DASD (**14**)], geminal disubstituted, N_3P_3(diazacrown)(amine)$_2Cl_2$ [amine; pyrrolidine (**9** and **11**)], and fully substituted, N_3P_3(diazacrown)(amine)$_4$ [amine; morpholine (**7** and **10**), and DASD (**8**)] phosphazene derivatives. The expected non-geminal (*cis*- or *trans*-) products could not have been isolated according to the reaction pathways [Scheme 2, (ii)]. In addition, fully

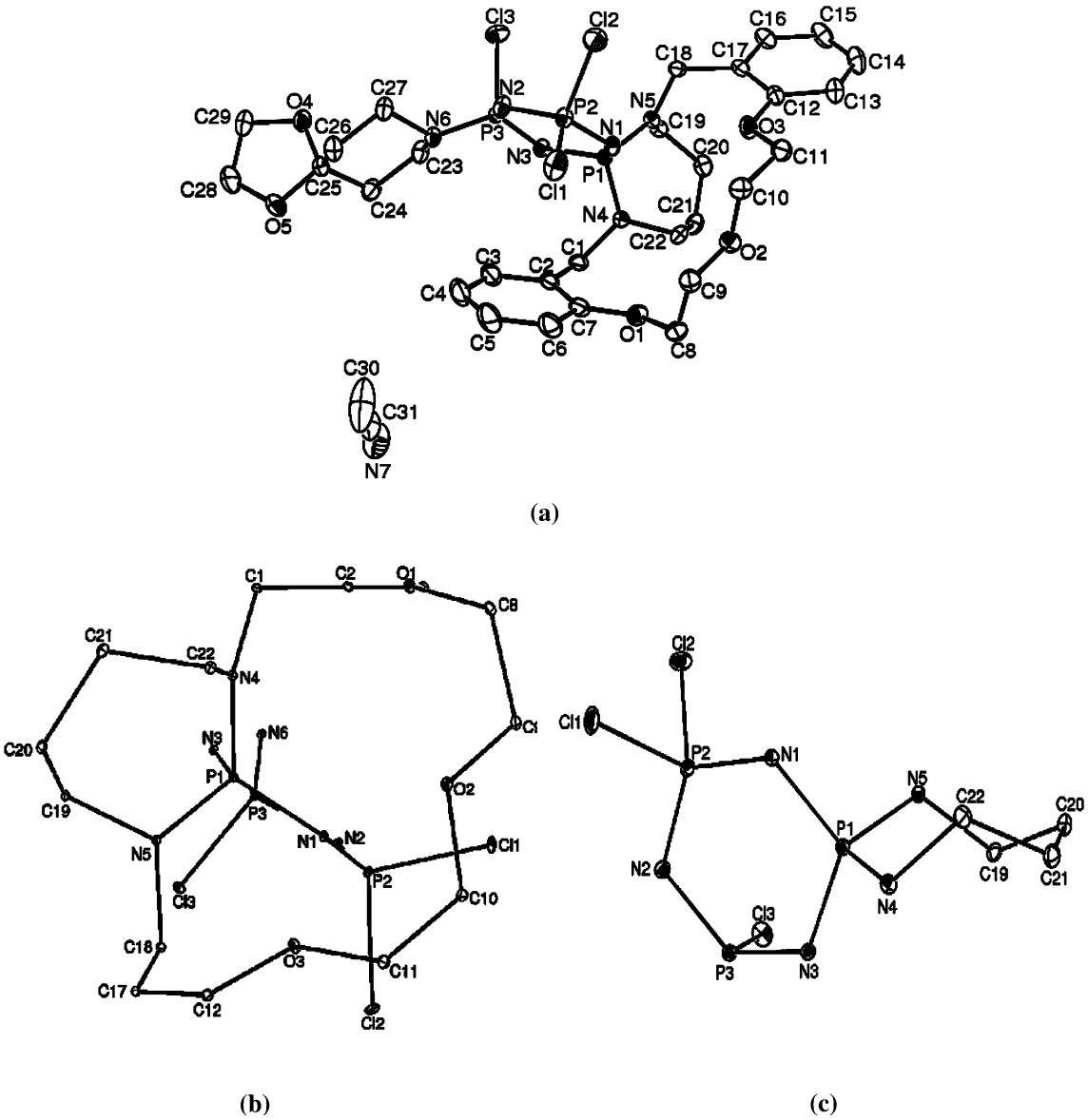

Fig. 3 **a** An ORTEP-3 [36] drawing of **14** with the atom-numbering scheme. Displacement ellipsoids are drawn at the 30% probability level. **b** The conformations of the phosphazene and the macrorings. **c** The conformation of the seven-membered *spiro*-ring

substituted phosphazene derivatives could not have also been isolated from the reactions of all the monotopic crypta-phosphazenes with excess pyrrolidine. Instead, the interesting geminal pyrrolidinyl substituted phosphazenes (**9** and **11**) are obtained. The geminal structures of **9** (Fig. 1) and the other analogous geminal pyrrolidinyl substituted phosphazenes have been determined by X-ray structure analyses [22]. In the literature, it is indicated that the secondary amines, e.g. pyrrolidine and diethyl amine show non-geminal bonding. However, in contrast to these observations, in (**9** and **11**) pyrrolidine show geminal bonding preference instead of non-geminal bonding [Scheme 2, (i)]. The possible reasons may be; (1) the macrocycle may hinder the attack of the pyrrolidine molecule to one of the $>PCl_2$ groups, and (2) there may be a mechanistic switch during the formations of **9** and **11**. But, geminal phosphazene derivatives of morpholine and DASD with **4**, **5** and **6** could not have been obtained in THF. Instead, mono and fully substituted products are separated from the reaction mixture.

Spectroscopic analyses

The FTIR spectra of all the phosphazene derivatives (**7**, **8** and **10**–**14**) exhibit two weak intensity absorption peaks at 3,070–3,064 and 3,034–3,021 cm^{-1} attributed to the asymmetric and symmetric stretching vibrations of the aromatic C–H protons, respectively. Monotopic

Table 1 Crystallographic data for compounds **9**, **13** and **14**

	(**9**)	(**13**)	(**14**)
Empirical formula	$C_{29}H_{42}Cl_2N_7O_3P_3$	$C_{26}H_{36}Cl_3N_6O_4P_3$	$C_{31}H_{43}Cl_3N_7O_5P_3$
Fw	700.51	695.87	793.00
Crystal system	Monoclinic	Monoclinic	Monoclinic
Space group	C 2/c	C 2/c	C 2/c
a (Å)	17.333(12)	30.9885(15)	22.5161(1)
b (Å)	17.853(5)	9.9642(5)	9.1716(2)
c (Å)	22.232(3)	21.8385(10)	36.7767(3)
α (°)	90.00	90.00	90.00
β (°)	95.91(2)	108.927(2)	107.389(10)
γ (°)	90.00	90.00	90.00
V (Å^3)	6843(5)	3365(2)	7247.61(17)
Z	8	8	8
μ (cm^{-1})	3.376 (Cu K_α)	0.481 (Mo K_α)	0.498 (Mo K_α)
ρ (calcd) (g cm^{-3})	1.360	1.449	1.454
Number of reflections total	3,355	42,298	7,540
Number of reflections unique	3,274	7,916	7,348
R_{int}	0.0470	0.0266	0.0241
$2\theta_{max}$ (°)	146.88	56.80	52.58
T_{min}/T_{max}	0.420/0.600	0.8498/0.9100	0.8632/0.9379
Number of parameters	397	379	431
R [$F^2 > 2\sigma(F^2)$]	0.0587	0.0353	0.0470
wR	0.0837	0.1043	0.1293

Table 2 The selected bond lengths (Å) and angles with the selected torsion angles (°) for **9**, **13** and **14**

(**9**)		(**13**)		(**14**)	
P1–N1	1.618(5)	P1–N1	1.615(1)	P1–N1	1.613(2)
P1–N3	1.586(4)	P1–N3	1.615(1)	P1–N3	1.614(2)
P1–N4	1.634(4)	P1–N4	1.637(2)	P1–N4	1.625(2)
P1–N5	1.642(5)	P1–N5	1.630(2)	P1–N5	1.627(2)
P2–N1	1.544(4)	P2–N1	1.565(1)	P2–N1	1.543(2)
P2–N2	1.560(4)	P2–N2	1.590(2)	P2–N2	1.563(2)
P3–N2	1.623(4)	P3–N2	1.567(2)	P3–N2	1.597(3)
P3–N3	1.573(4)	P3–N3	1.557(1)	P3–N3	1.559(2)
P3–N6	1.649(4)	P2–Cl3	2.073(8)	P3–N6	1.631(2)
P3–N7	1.649(5)	P3–Cl1	2.025(6)	P3–Cl3	2.074(1)
N1–P1–N3	115.6(2)	N1–P1–N3	113.1(7)	N1–P1–N3	112.5(1)
N1–P1–N4	111.5(2)	N1–P1–N4	114.9(8)	N1–P1–N4	114.5(1)
N1–P1–N5	105.4(2)	N1–P1–N5	105.6(8)	N1–P1–N5	106.5(1)
N3–P1–N4	105.5(2)	N3–P1–N4	106.3(8)	N3–P1–N4	105.1(1)
N3–P1–N5	113.1(2)	N3–P1–N5	114.1(8)	N3–P1–N5	116.0(1)
N4–P1–N5	105.4(2)	N4–P1–N5	102.6(7)	N4–P1–N5	102.2(1)
N1–P2–N2	121.3(2)	N1–P2–N2	120.0(8)	N1–P2–N2	121.3(1)
N2–P3–N3	113.5(2)	N2–P3–N3	120.6(8)	N2–P3-N3	119.3(1)
N2–P3–N6	110.0(2)	P3–N2–P2	117.1(9)	P3–N2–P2	116.9(2)
N2–P3–N7	109.0(2)	P3–N3–P1	123.4(9)	P3–N3–P1	122.4(2)
N3–P3–N6	110.8(2)	P2–N1–P1	121.4(9)	P2–N1–P1	123.5(1)
N3–P3–N7–C12	70.4(5)	N3–P1–N5–C5	92.54(15)	N1–P1–N4–C1	93.6(2)
N3–P3–N6–C29	58.3(4)	N1–P1–N4–C22	94.62(14)	N3–P1–N5–C18	101.3(2)

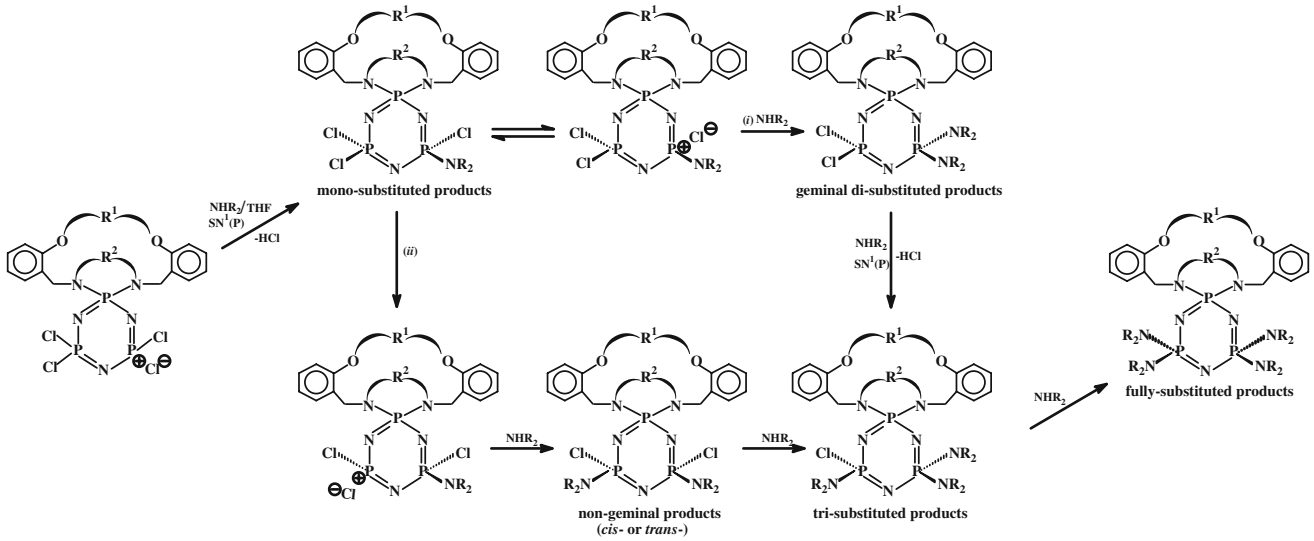

Scheme 2 The reaction pathway of monotopic-*spiro* crypta phosphazenes with secondary amines in THF

Table 3 ^{31}P-NMR Data in $CDCl_3$ (δ in ppm, J in Hz)

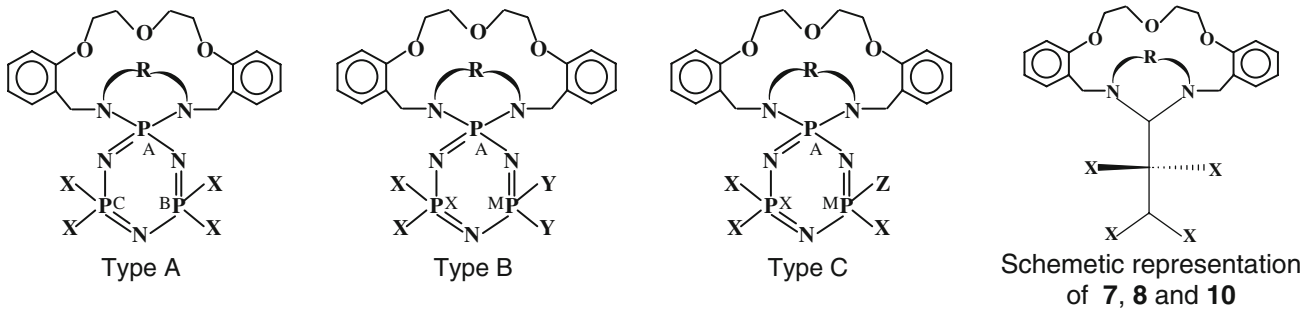

Compound	Spin system	δPN_2	δPX_2	δPY_2	δPXZ	$^2J_{PP}$
7	ABC	P_A:22.90	P_B:23.05 P_C:23.04	–	–	$^2J_{AB}$:55.5 $^2J_{AC}$:53.5 $^2J_{BC}$:22.9
8	ABC	P_A:20.80	P_B:23.10 P_C:22.30	–	–	$^2J_{AB}$:49.2 $^2J_{AC}$:31.9 $^2J_{BC}$: ~0
10	ABC	P_A:20.05	P_B:23.94 P_C:21.04	–	–	$^2J_{AB}$:51.5 $^2J_{AC}$:51.1 $^2J_{BC}$:28.6
11	AMX	P_A:18.29	P_X:23.68	P_M:14.38	–	$^2J_{MX}$:54.1 $^2J_{AM}$:43.4 $^2J_{AX}$:43.0
12	AMX	P_A:15.79	P_X:21.11	–	P_M:24.77	$^2J_{MX}$:56.9 $^2J_{AX}$:47.5 $^2J_{AM}$:41.1
13	AMX	P_A:16.06	P_X:21.39	–	P_M:25.03	$^2J_{MX}$:58.8 $^2J_{AM}$:46.9 $^2J_{AX}$:41.9
14	AMX	P_A:16.02	P_X:21.25	–	P_M:25.05	$^2J_{MX}$:59.6 $^2J_{AM}$:47.2 $^2J_{AX}$:42.7

P_B and P_C values of **7**, **8** and **10** may be reversed

crypta-phosphazenes display intense stretching bands between 1,234–1,229 and 1,196–1,181 cm^{-1}, attributed to $\nu_{P=N}$ bonds of phosphazene skeleton. As expected, two kinds of ν_{P-Cl} absorption peaks have arisen for the partially substituted phosphazenes (**9** and **11–14**) at 577–552 and 525–482 cm^{-1}. The peaks at 3,456 cm^{-1} for **7** and 2,225 cm^{-1} for **14** indicate that these compounds contain H_2O and CH_3CN molecules.

The ^{1}H-decoupled ^{31}P NMR data of the phosphazenes are listed in Table 3. The spin systems of the compounds are interpreted as simple ABC and AMX from the ^{31}P NMR spectra of (**7**, **8** and **10**) and (**11–14**), respectively. The proton coupled ^{31}P NMR spectra of **9** [19] and **11** indicate that only geminal-geometric isomers are isolated. In **7**, **8** and **10**, the substituents R and R′ (Table 6) appear to project sideways, and thus the two >P(amine)$_2$ groups are in different environments which leads to an asymmetry. Because R and R′ differ, anisochrony [19, 22] has arisen for the two >P(amine)$_2$ groups. Therefore, the ^{31}P-NMR spectra of **7**, **8** and **10** do not contain any doublet and triplet for the two P(amine)$_2$ and P_{spiro} phosphorus atoms, due to the anisochrony (Fig. 4). On the other hand, the mono substituted compounds **12**, **13** and **14** have a typical 12 lines resonance pattern consisting of three doublets of doublet for δP_{spiro} (15.80 ppm for **12**, 16.06 ppm for **13**, and 16.02 ppm for **14**) δPCl_2 (21.11 ppm for **12**, 21.39 ppm for **13** and 21.25 for **14**), and δP(amine)Cl (24.77 ppm for 1**2**, 25.03 ppm for **13** and 25.05 ppm for **14**). The signals of the δP(amine)Cl values of **12**, **13** and **14** are lowfield-shifted by 3.21 ppm for **12**, 3.47 ppm for **13**, and 3.49 ppm for **14**, with respect to the corresponding PCl_2 group of the starting compound [22]. Two P atoms of **12**, **13** and **14** are stereogenics, because they have four different substituents. Hence, they have RR, SS, RS and SR configurations. Due to the presence of two stereogenic centers in compounds **12–14** one would expect the occurrence of diastereomers which should give rise to distinguishable NMR signals. Table 3 lists only a single set of signals. The stereogenic properties of the phosphazene derivatives are observed by ^{31}P-NMR spectroscopy on addition of a chiral solvating agent (CSA) [27]. On addition of CSA, the ^{31}P-NMR signals of the stereogenic compounds may split into two lines indicating that they exist as diastereomers.

In the crypta phosphazene architectures, the ^{1}H and ^{13}C NMR peaks have been assigned on the basis of chemical shifts, multiplicities and coupling constants. The assignments have been made unambiguously by DEPT and HETCOR using the values corresponding to $^1J_{CH}$ between carbons and protons (Table 4). The DEPT and HETCOR spectra of **14** are illustrated in Figs. 5b and 6, as an example and all of the ^{1}H and ^{13}C NMR assignments have been marked on the spectra. According to the ^{1}H and ^{13}C NMR data of **7**, **8** and **10**, these molecules seem to have symmetric structures in solution. All of the compounds

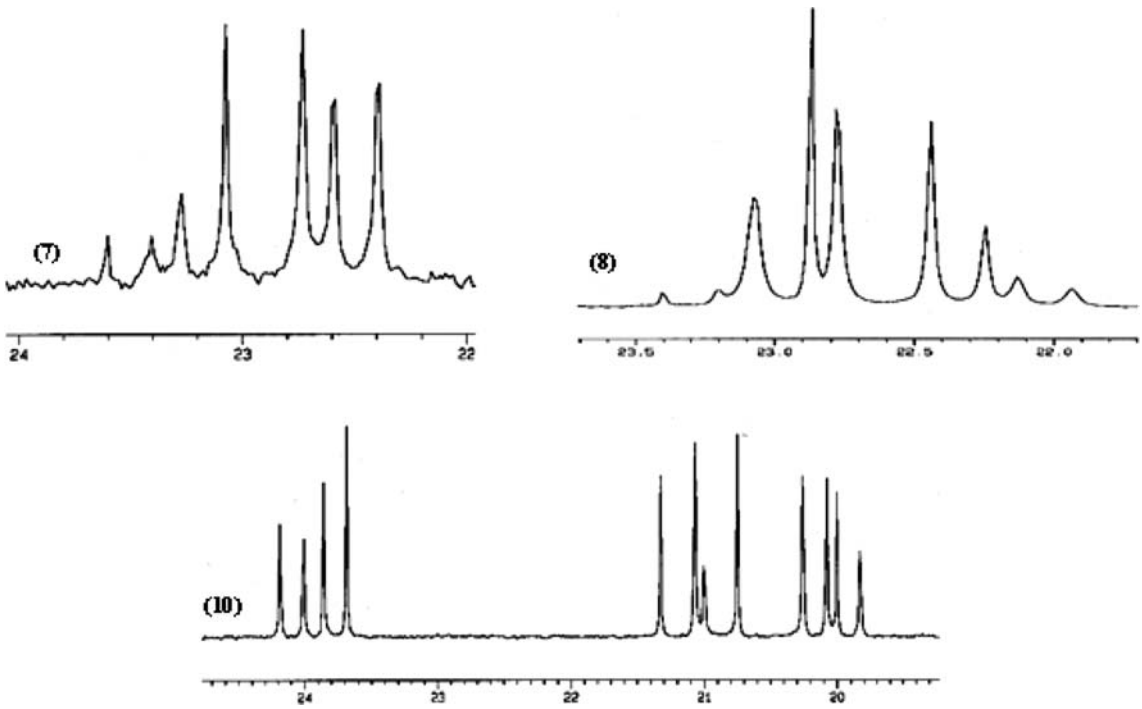

Fig. 4 ^{31}P-NMR spectra of **7**, **8** and **10** showing anisochronism

Table 4 ^{1}H-NMR data for **7**, **8**, **10**, **11**, **12**, **13** and **14**

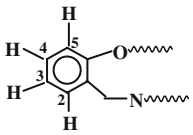

	7	**8**	**10**	**11**	**12**	**13**	**14**
H_2	6.83 $^{3}J_{H2–H3} = 8.2$ $^{4}J_{H2–H4} = 1.7$	6.80 $^{3}J_{H2–H3} = 8.1$ $^{4}J_{H2–H4} = 1.7$	6.91 $^{3}J_{H2–H3} = 7.5$ $^{4}J_{H2–H4} = 1.5$	6.83 $^{3}J_{H2–H3} = 7.8$ $^{4}J_{H2–H4} = 1.7$	6.85 $^{3}J_{H2–H3} = 7.7$ $^{4}J_{H2–H4} = 1.8$	6.84 $^{3}J_{H2–H3} = 8.1$ $^{4}J_{H2–H4} = 1.5$	6.85 $^{3}J_{H2–H3} = 7.5$ $^{4}J_{H2–H4} = 1.6$
H_3	6.85 $^{3}J_{H3–H4} = 7.9$ $^{3}J_{H2–H3} = 8.2$ $^{4}J_{H3–H5} = 1.5$	6.87 $^{3}J_{H3–H4} = 7.8$ $^{3}J_{H2–H3} = 8.1$ $^{4}J_{H3–H5} = 1.6$	7.03 $^{3}J_{H3–H4} = 7.4$ $^{3}J_{H2–H3} = 7.5$	6.87 $^{3}J_{H3–H4} = 7.6$ $^{3}J_{H2–H3} = 7.8$ $^{4}J_{H3–H5} = 1.5$	6.90 $^{3}J_{H3–H4} = 7.4$ $^{3}J_{H2–H3} = 7.7$ $^{4}J_{H3–H5} = 1.6$	6.90 $^{3}J_{H3–H4} = 7.6$ $^{3}J_{H2–H3} = 8.1$ $^{4}J_{H3–H5} = 1.5$	6.90 $^{3}J_{H3–H4} = 7.3$ $^{3}J_{H2–H3} = 7.5$ $^{4}J_{H3–H5} = 1.5$
H_4	7.26 $^{3}J_{H4–H5} = 7.4$ $^{4}J_{H2–H4} = 1.7$ $^{3}J_{H3–H4} = 7.9$	7.30 $^{3}J_{H4–H5} = 7.4$ $^{4}J_{H2–H4} = 1.7$ $^{3}J_{H3–H4} = 7.8$	7.23 $^{3}J_{H4–H5} = 6.3$ $^{4}J_{H2–H4} = 1.5$ $^{3}J_{H3–H4} = 7.4$	7.26 $^{3}J_{H4–H5} = 7.1$ $^{4}J_{H2–H4} = 1.7$ $^{3}J_{H3–H4} = 7.6$	7.28 $^{3}J_{H4–H5} = 6.3$ $^{4}J_{H2–H4} = 1.8$ $^{3}J_{H3–H4} = 7.4$	7.29 $^{3}J_{H4–H5} = 7.1$ $^{4}J_{H2–H4} = 1.5$ $^{3}J_{H3–H4} = 7.6$	7.30 $^{3}J_{H4–H5} = 6.5$ $^{4}J_{H2–H4} = 1.6$ $^{3}J_{H3–H4} = 7.3$
H_5	7.17 $^{4}J_{H3–H5} = 1.5$ $^{3}J_{H4–H5} = 7.4$	7.22 $^{4}J_{H3–H5} = 1.6$ $^{3}J_{H4–H5} = 7.4$	7.28 $^{3}J_{H4–H5} = 6.3$	7.17 $^{4}J_{H3–H5} = 1.5$ $^{3}J_{H4–H5} = 7.1$	7.28 $^{4}J_{H3–H5} = 1.6$	7.24 $^{4}J_{H3–H5} = 1.5$ $^{3}J_{H4–H5} = 7.1$	7.20 $^{4}J_{H3–H5} = 1.5$ $^{3}J_{H4–H5} = 6.5$
N–CH_2–CH_2	–	*d*:1.65(m,16H)	1.45(m,1H) 1.80(m,1H)	1.60(m,4H) *p*:1.90(m,8H)	1.25(m,2H) 1.30(m,2H) *p*:2.00(m,4H)	0.90(m,2H) 1.30(m,2H)	0.54(m,2H) 0.94(m,2H) *d*:1.87(t,4H) $^{2}J_{HH} = 5.2$
N–CH_2	3.20(m,4H) *m*:2.69(m,16H)	2.63(d,4H) $^{3}J_{PH} = 15.6$ *d*:3.28(m,16H)	3.45(m,4H) *m*:3.00(m,8H) *m*:3.20(m,8H)	3.20(m,4H) *p*:3.30(m,8H)	3.15(m,1H) 3.45(m,3H) $^{3}J_{PH} = 14.6$ *p*:3.35(m,3H) *p*:3.60(m,1H) $^{3}J_{PH} = 6.5$	3.20(m,2H) 3.40(m,2H) *m*:3.30(m,4H)	3.58(m,2H) 3.60(m,2H) *d*:3.37(m,64H)
Ar–CH_2–N	3.65(m,2H) 4.50(m,2H)	3.60(d,2H) $^{3}J_{PH} = 11.8$ Hz 4.55(d,2H) $^{3}J_{PH} = 11.8$ Hz	3.40(m,2H) 4.55(q,2H) $^{2}J_{HH} = 7.8$ $^{3}J_{PH} = 14.5$	3.75(m,2H) 4.80(q,2H) $^{2}J_{HH} = 8.7$ $^{3}J_{PH} = 13.4$	3.68(q,1H) $^{3}J_{PH} = 12.7$ 3.75(q,1H) $^{2}J_{HH} = 9.4$ $^{3}J_{PH} = 14.1$ 4.55(q,1H) $^{3}J_{PH} = 13.8$ $^{2}J_{HH} = 8.4$ 4.94(q,1H) $^{3}J_{PH} = 13.3$	3.70(m,2H) 4.40(m,2H)	3.70(m,2H) 4.36(q,2H) $^{3}J_{PH} = 10.0$
O–CH_2–CH_2	3.70(m,2H) 4.14(m,2H)	4.18(m,2H) 3.45(m,2H)	4.30(m,2H) 3.90(m,2H)	4.35(m,4H)	3.65(m,2H) 4.10(m,2H)	3.68(m,2H) 4.17(m,2H)	4.15(m,2H) 3.65(m,2H)
O–CH_2	4.50(m,4H) *m*:3.70(m,16H)	4.38(m,4H) *d*:3.95(m,16H)	4.06(m,2H) 4.11(m,2H) *m*:3.73(m,8H) 3.45(m,8H)	3.80(m,2H) 4.15(m,2H)	4.20(m,2H) 4.35(m,2H)	4.52(m,2H) 4.90(m,2H) *m*:3.76(m,4H)	4.35(m,2H) 4.20(m,2H) *d*:4.02(m,4H)

δ are reported in ppm, J values in Hz

d DASD, *m* morpholine, *p* pyrrolidine, *s* singlet, *d* doublet, *t* triplet, *q* quartet, *m* multiplet

give very complex ^{1}H NMR spectra, since the aliphatic protons are not equivalent to each other. The benzylic Ar-CH_2 diastrotopic protons are highly separated from each other and can easily be distinguished by using HETCOR; one of the peak groups is in the range of δ 3.40–3.70 ppm, whilst the other is in the range of δ 4.10–4.55 ppm. These protons give generally quartets, because of the $^2J_{HH}$ and $^3J_{PH}$ couplings, as expected from *P*NCH_2-precursor. On the other hand, the signals of the non-protonated carbon atoms disappear in DEPT spectrum of **14** as compared with the ^{1}H decoupled ^{13}C NMR spectrum (Fig. 5a, b). So, in compounds **8** and **14**, the δ values of *spiro* carbons of DASD are assigned at 107.7 and 105.0 ppm, respectively. In addition, the $^2J_{PC}$ values of Ar-*C*H_2 of seven membered *spiro*-crypta phosphazenes, **13** and **14**, are larger than the five membered *spiro*-crypta phosphazene, **8**. While, the $^2J_{PC}$ values of N–*C*H_2 of five membered *spiro*-crypta phosphazenes, **7** and **8**, are highly larger than those of seven membered ones, **13** and **14** (Table 5)

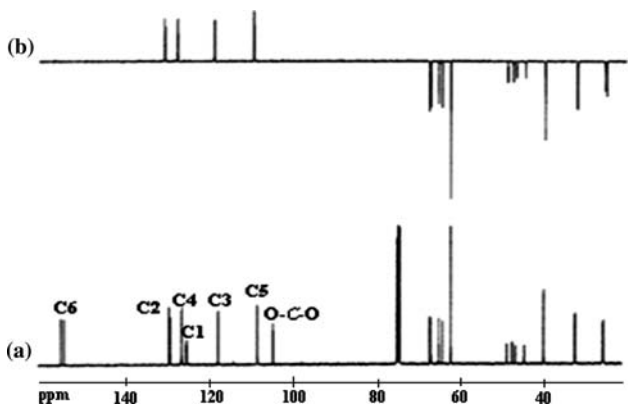

Fig. 5 **a** The ^{13}C-NMR and **b** DEPT spectra of compound **14**

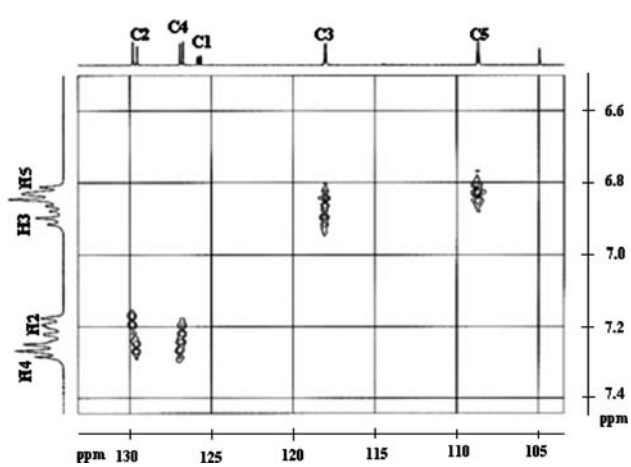

Fig. 6 The HETCOR spectrum of **14**

X-Ray analyses of **9**, **13** and **14**

In order to further corroborate the structural assignments, single crystal X-ray structures of compounds **9**, **13** and **14** are reported. Their molecular structures are given in Figs. 1a, 2a and 3a, respectively. Their phosphazene rings are not planar, and are in flattened-boat [Fig. 1b; $\phi_2 = -171.88(1.92)°$ and $\theta_2 = 142.59(1.04)°$], twisted [Fig. 2b; $\phi_2 = -84.52(90)°$ and $\theta_2 = 152.03(40)°$] and twisted [Fig. 3b; $\phi_2 = -93.22(1.40)°$ and $\theta_2 = 29.00(56)°$] conformations having total puckering amplitudes Q_T of 0.153(3) Å, 0.176(1) Å and 0.171(2) Å, respectively.

In **9**, the six-membered ring (P3/N6/N7/C9–C11) is in chair conformation [Fig. 1c; $Q_T = 0.936(1)$ Å, $\phi_2 = -26.3(9)°$ and $\theta_2 = 124.4(3)°$]. In **13**, the seven-membered ring (P1/N4/N5/C1–C4) is in twisted conformation [Fig. 2c; $Q_T = 1.277(3)$ Å, $\phi_2 = -49.5(1)°$, $\phi_3 = -161.6(2)°$ and $\theta_2 = 44.3(1)°$]. In **14**, the seven-membered ring (P1/N4/N5/C19–C22) is also in twisted conformation [Fig. 3c; $Q_T = 0.866(3)$ Å, $\phi_2 = 117.8(3)°$, $\phi_3 = 75.8(2)°$ and $\theta_2 = 34.9(2)°$]. As expected, none of the macrocyclic rings are planar with the puckering amplitudes Q_T of 1.488(8) Å (for **9**), 1.876(2) Å (for **13**) and 1.930(3) Å (for **14**).

The average P–N bond lengths in phosphazene rings of **9**, **13** and **14** are 1.584(4), 1.585(2), and 1.582(2) Å, which are shorter than the average exocyclic P–N bonds of 1.644(5), 1.632(2) and 1.628(2) Å for **9**, **13** and **14**, respectively. The sum of the bond angles around the N atoms in the six- and seven-membered *spiro*-cyclic rings are [344.8(4)° and 347.6(4)°] for **9**, [357.2(1) and 359.3(1)°] for **13** and [359.8(2)° and 358.0(2)°] for **14**, which approve that the N atoms in **9** have pyramidal geometries. Hence, they may have stereogenic configurations, as in compound **4** [24]. As can be seen from Table 2; in **9**, the α (N2–P3–N3) [113.5(2)°] and γ (N1–P1–N3) [115.6(2)°] angles are narrowed, while β (P1–N3–P3) [125.3(3)°] angle is highly expanded, considerably with respect to the corresponding values in "standard" compound $N_3P_3Cl_6$. In $N_3P_3Cl_6$, the α, α', γ, γ', β and δ angles are 118.3(2)°, 101.2(1)°, 118.3(2)°, 101.2(1)°, 121.4(3)° and 121.4(3)°, respectively [37]. The narrowing in the α and γ angles imply that strong electron back-donation to the N_3P_3 phosphazene rings have occurred from the exocyclic N atoms and pyrrolidine rings. The electron back-donation also causes to the shortening of the exocyclic P–N bonds. In **13**, α (N1–P1–N3) [113.13(7)°] and δ (P2–N2–P3) [117.13(9)°] angles are narrowed, while γ (N1–P2–N2) [120.00(8)°] and γ' (Cl3–P2–N6) [104.78(7)°] angles are expanded as in compound **14**, where α, δ, γ and γ' angles are 112.46(12)°, 116.90(16)°, 119.30(13)° and 104.15(10)°, respectively.

The inner hole-sizes of the macrocycles in radii of **9**, **13** and **14**, estimated as twice the mean distances of the donor atoms from their centroids, are approximately 1.73 Å (for **9**), 1.53 Å (for **13**) and 1.58 Å (for **14**) using the 'modified

Table 5 ^{13}C-NMR (decoupled) spectral data for **7**, **8**, **10**, **11**, **12**, **13** and **14**

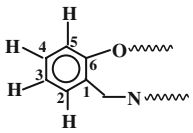

	7	**8**	**10**	**11**	**12**	**13**	**14**
C_1	125.3 $^3J_{PC} = 9.2$	126.0 $^3J_{PC} = 8.8$	125.3 $^3J_{PC} = 11.0$	127.8 $^3J_{PC} = 7.0$	127.8 $^3J_{PC} = 7.1$ 127.7 $^3J_{PC} = 7.3$	127.6 $^3J_{PC} = 11.0$ 127.5 $^3J_{PC} = 7.3$	125.7 $^3J_{PC} = 7.1$ 125.8 $^3J_{PC} = 3.8$
C_2	131.9	132.0	130.5	131.2	131.7 131.5	131.8 131.5	129.8 129.6
C_3	120.3	120.1	121.0	119.9	120.3 119.9	120.1 119.8	118.1 117.9
C_4	129.2	128.9	128.3	128.7	128.6 128.8	128.6 128.8	126.9 126.7
C_5	111.3	111.3	114.0	110.0	110.7 110.8	110.6 110.8	108.6 108.7
C_6	158.0	158.1	157.5	157.9	157.7 157.0	157.7 157.0	155.0 155.7
N–CH_2–CH_2	–	*d*: 35.8	30.3	27.7 *p*: 26.4 $^3J_{PC} = 9.3$	27.8; 28.2 *p*: 26.0 $^3J_{PC} = 11.0$	29.7; 28.2	26.3; 25.9 *d*: 32.8; 32.7 $^3J_{PC} = 10.6$
N–CH_2	44.9 $^2J_{PC} = 18.3$ *m*: 42.3; 42.5	42.8 $^2J_{PC} = 12.3$ *d*: 42.3	46.2 *m*: 44.9	45.8 $^2J_{PC} = 6.1$ *p*: 46.2 $^2J_{PC} = 4.2$	49.0 $^2J_{PC} = 7.0$ 46.6 $^2J_{PC} = 6.7$ *p*: 46.8 $^2J_{PC} = 2.6$	49.0 $^2J_{PC} = 7.4$ 46.9 $^2J_{PC} = 7.1$ *m*: 43.9	47.1 $^2J_{PC} = 7.0$ 45.0 $^2J_{PC} = 6.6$ *d*: 40.3
Ar–CH_2–N	46.0	45.8 $^2J_{PC} = 3.1$	46.8	49.7 $^2J_{PC} = 7.9$	49.7 $^2J_{PC} = 7.9$ 51.0 $^2J_{PC} = 7.4$	51.2 $^2J_{PC} = 7.4$ 49.8 $^2J_{PC} = 7.8$	47.9 $^2J_{PC} = 7.9$ 49.2 $^2J_{PC} = 7.5$
O–CH_2–CH_2	69.8	69.9	69.8	69.6	69.2; 69.6	69.5; 69.2	67.2; 67.6
O–CH_2	68.4 *m*: 67.4 $^3J_{PC} = 8.2$	66.3	69.6 *m*: 67.3 $^3J_{PC} = 11.0$ 67.4 $^3J_{PC} = 11.0$	67.7	67.4; 66.6	67.3; 66.5 *m*: 66.6 $^3J_{PC} = 11.8$	64.5; 65.3 *d*: 62.5
O–*C*–O	–	*d*: 107.7	–	–	–	–	105.0 $^4J_{PC} = 1.8$

δ are reported in ppm, J values in Hz

d DASD, *m* morpholine, *p* pyrrolidine

covalent radii' of the N^2_{sp} (0.66 Å), N^3_{sp} (0.72 Å) and O^3_{sp} (0.76 Å) atoms, as in the literature method [38]. Compound **14** also contains the acetonitrile molecules forming caviplex [39], as depicted in the packing diagram of **14** (Fig. 7). Dipole–dipole and van der Waals forces may be effective in holding the acetonitrile molecules in the cavities.

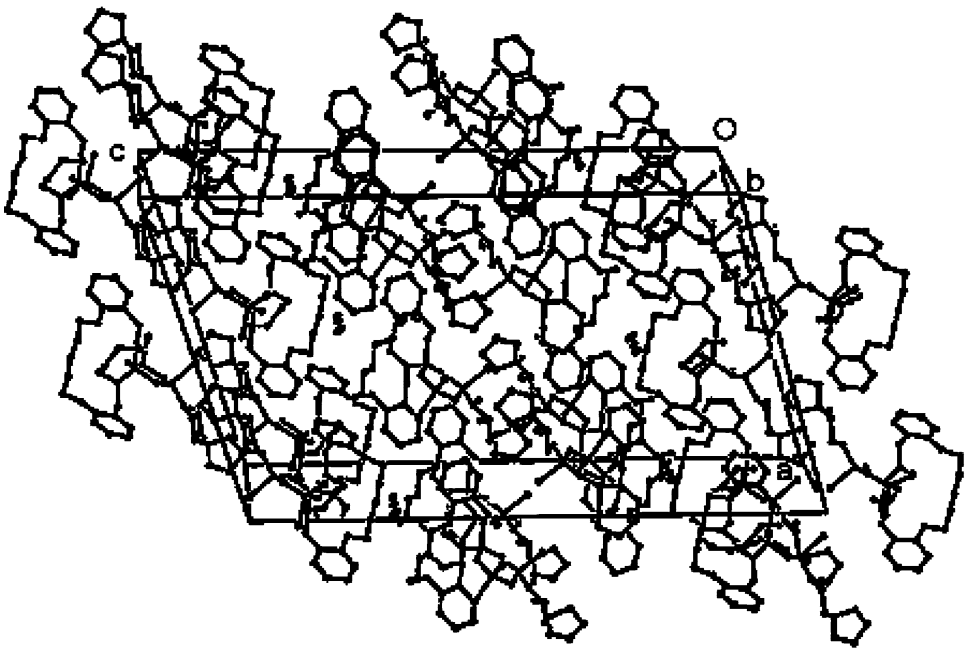

Fig. 7 A packing diagram of compound **14**

The relationship between ^{31}P NMR spectral and X-ray crystallographic data

A systematic study of crystallographic data has revealed correlations between structural parameters in four kinds of analogous phosphazenes synthesized by our research group (Table 6). The first group members are *spiro*-crypta phosphazenes (type A). Pyrrolidine (type B), morpholine and DASD (type C) substituted *spiro*-crypta phosphazenes are the second and the third group members, respectively. Ditopic *spiro*-crypta phosphazenes (type D) constitute the fourth group. Using the bond angles (α and α') and the bond lengths (a and b) of phosphazene ring, it is observed a number of relationships which can be gained from ^{31}P NMR spectral and X-ray crystallographic data. These include (1) exocyclic (α') and endocyclic (α) NPN bond angles versus $\delta P_{A(spiro)}$-shifts (Fig. 8) and (2) electron density transfer parameters Δ(P–N) [Δ(a–b): the difference between the bond lengths of two adjacent P–N bonds] and their relationships to both $\Delta(\delta P)$ and δP_A-shifts (Fig. 9). The NPN bond angles (α and α') and bond lengths (a, a′, b and b′) on the general formulae of the phosphazenes are marked and δP-shifts, Δ(P–N) and $\Delta(\delta P)$ values that are needed to be used for graph construction are listed in Table 6. In phosphazene derivatives, the variations in the bond angles depend on the steric and electronic factors (for example the conformation and electron releasing and the withdrawing capacities of small or bulky substituents and the steric hinderences of exocyclic groups) [19, 40]. The variations of δP-shifts depend essentially on the variations of the angles around the phosphorus atoms and especially on the variations of α- and α'-angles. In Fig. 8a showing the correlations between δP_A shifts and exocyclic NPN (α') bond angles, it has been found that relatively small changes in exocyclic bond angles were shown to cause large changes in δP_A-shifts. On the left hand side of the curve, the five membered crypta rings (**1** and **4**) are accumulated, while the six and seven membered ones are accumulated on the right hand side of the curve. Moreover, a "cluster" of points rather than a trend of the linearity has been observed between δP_A-shifts and the endocyclic (α) NPN bond angles (Fig. 8b). In Fig. 8b, one can easily observe two separate regions (A and B). It is observed that the points of types A and C phosphazenes and types B and D phosphazenes are accumulated in regions A and B, respectively (Fig. 8b). The order of α-values are; $N_3P_3Cl_6$ [37] > the phosphazenes in region B cycle > the phosphazenes in region A cycle. On the other hand, the relationship between the Δ(P–N) values and δP_A or $\Delta(\delta P)$ shifts are illustrated in Fig. 9. Electron density transfer parameter Δ(P–N) indicates the measure of electron releasing and withdrawing capacities of the substituents bonded to the phosphazene ring [41], Δ(P–N) values are calculated from the equations given in Table 6 for four different types of phosphazenes. When Δ(P–N) values are increasing, the substituents bonding to phosphazene ring withdraw electrons from the ring. On the other hand, when this value is decreasing, substituents bonding to phosphazene ring release electrons to the ring. In addition, the shortening of the endocyclic P–N bonds is likely to be a measure of these properties. In Fig. 9a, the points also seem as a "cluster". The electron releasing powers of the pyrrolidine substituents are more effective than those of the *spiro*-rings. Therefore, the electron releasing powers of the types B and D in region B cycle are greater than those of

Table 6 NPN bond angles (α and α′), bond lengths (a, a′, b and b′), δP-shifts, Δ(P–N) and Δ(δP) values for the compounds [δP values are reported in ppm, α and α′ angles in (°)]

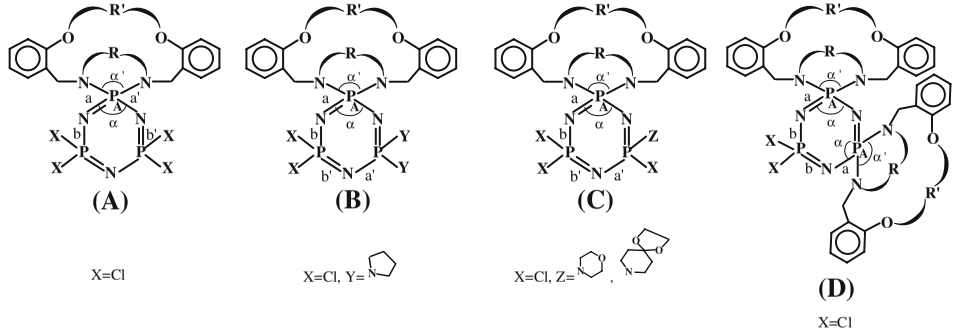

$$\Delta(\delta P) = \frac{\delta P_{X2} + \delta P_{X2}}{2} - \delta P_A \text{ for type (A)}$$

$$\Delta(\delta P) = \frac{\delta P_{X2} + \delta P_{YZ}}{2} - \delta P_A \text{ for type (B)}$$

$$\Delta(\delta P) = \delta P_{X2} - \delta P_A \text{ for types (C) and (D)}$$

$$\Delta(\text{P-N}) = \frac{a + a'}{2} - \frac{b + b'}{2} \text{ for types (A), (B) and (C)}$$

$$\Delta(\text{P-N}) = a - b \text{ for type (D)}$$

Type	R	R′	Comp.	a	a′	b	b′	Δ(P–N)	δP_X	δP_A	Δ(δP)	Δ(P–N): δP_A	Δ(P–N): Δ(δP)	NPN(α′):δP_A	NPN(α):δP_A
(**A**)	$(CH_2)_2$	$(CH_2)_3$	(**I**)[16]	1.6267(19)	1.6020(19)	1.5597(19)	1.5598(19)	0.0546	21.12, 25.52	15.30	8.02	0.0546:15.30	0.0546:8.02	95.22:15.30	111.78:15.30
	$(CH_2)_2$	$(CH_2–CH_2)_2O$	(**4**)[17,18]	1.598(4)	1.622(4)	1.562(4)	1.553(4)	0.0525	23.58, 24.46	15.50	9.02	0.0525:15.50	0.0525:9.02	95.43:15.50	111.60:15.50
	$(CH_2)_3$	$(CH_2)_2$	(**II**)[19]	1.6008(16)	1.6287(16)	1.5633(16)	1.5525(15)	0.05685	17.51, 22.72	14.20	5.95	0.05685:14.20	0.05685:5.95	105.33:14.20	114.24:14.20
	$(CH_2)_3$	$(CH_2)_3$	(**III**)[20]	1.616(2)	1.597(2)	1.542(2)	1.5482(19)	0.0614	17.52, 24.71	13.71	7.405	0.0614:13.71	0.0614:7.405	103.05:13.71	111.76:13.71
	$(CH_2)_3$	$(CH_2)_4$	(**IV**)[21]	1.602(3)	1.626(3)	1.546(3)	1.536(3)	0.073	19.35, 25.30	15.25	7.075	0.073:15.25	0.073:7.075	103.69:15.25	112.50:15.25
	$(CH_2)_3$	$(CH_2–CH_2)_2O$	(**5**)[17]	1.611(4)	1.595(4)	1.562(4)	1.558(5)	0.043	19.58, 23.50	17.15	4.39	0.043:17.15[a]	0.043:4.39[a]	104.9:17.15	111.8:17.15
				1.639(5)	1.600(5)	1.548(5)	1.554(5)	0.0685				0.0685:17.15	0.0685:4.39	104.7:17.15	112.6:17.15
	$(CH_2)_4$	$(CH_2)_3$	(**V**)[22]	1.610(2)	1.622(2)	1.5476(19)	1.545(2)	0.06965	18.67, 19.96	15.31	4.305	0.06965:15.31	0.06965:4.305	106.35:15.31	111.88:15.31
	$(CH_2)_4$	$(CH_2)_4$	(**VI**)[22]	1.626(2)	1.617(2)	1.546(2)	1.549(2)	0.074	19.07, 20.26	14.06	5.605	0.074:14.06	0.074:5.605	103.39:14.06	112.32:14.06
(**B**)	$(CH_2)_3$	$(CH_2)_3$	(**VII**)[22]	1.603(3)	1.620(3)	1.562(3)	1.545(3)	0.058	27.20	18.33	8.87	0.058:18.33	0.058:8.87	100.62:18.33	114.35:18.33
	$(CH_2)_3$	$(CH_2)_4$	(**VIII**)[20,23]	1.6020(15)	1.6206(15)	1.5720(15)	1.5594(15)	0.0456	26.74	18.86	7.88	0.0456:18.86	0.0456:7.88	103.6:18.86	116.51:18.86
	$(CH_2)_3$	$(CH_2–CH_2)_2O$	(**9**)	1.623(4)	1.618(5)	1.560(4)	1.544(4)	0.0685	22.87	19.95	2.92	0.0685:19.95	0.0685:2.92	102.6:19.95	113.5:19.95
(**C**)	$(CH_2)_4$	$(CH_2–CH_2)_2O$	(**13**)	1.6152(14)	1.5896(16)	1.5565(14)	1.5670(15)	0.04065	21.39, 25.03	16.06	7.15	0.04065:16.06	0.04065:7.15	102.55:16.06	113.13:16.06
	$(CH_2)_4$	$(CH_2–CH_2)_2O$	(**14**)	1.613(2)	1.597(3)	1.543(2)	1.563(2)	0.0625	21.25, 25.05	16.02	7.13	0.0625:16.02	0.0625:7.13	102.16:16.02	112.46:16.02
(**D**)	$(CH_2)_3$	$(CH_2)_3$	(**IX**)[23]	1.5966(19)	–	1.5705(19)	–	0.0261	29.70	17.58	12.12	0.0261:17.58	0.0261:12.12	101.03:17.58	115.01:17.58
				1.6363(19)	–	1.5591(18)	–	0.0772				0.0772:17.58[a]	0.0772:12.12[a]	101.36:17.58	114.52:17.58
	$(CH_2)_3$	$(CH_2)_4$	(**X**)[23]	1.597(3)	–	1.548(3)	–	0.049	28.90	18.50	10.4	0.049:18.50[a]	0.049:10.4[a]	100.75:18.50	113.45:18.50
				1.600(3)	–	1.560(3)	–	0.040				0.040:18.50	0.040:10.4	100.35:18.50	113.96:18.50

[a] The point has not been taken into account for graph construction

Table 7 Substituent effect on electron releasing to N_3P_3 ring

Substituent	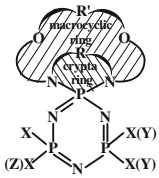				The order of electron releasing power
Macrocycly ring	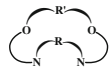 Skeletal structure	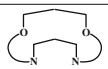 16-membered (IX)	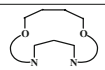 17-membered (X)		(IX) > (X)
		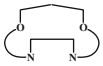 15-membered (II)	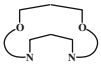 16-membered (III)	 17-membered (IV)	(II) > (III) > (IV)
		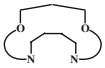 17-membered (V)	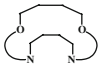 18-membered (VI)		(V) > (VI)
Crypta ring	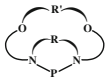 Skeletal structure	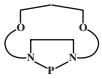 5-membered (I)	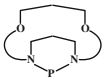 6-membered (III)	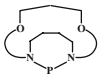 7-membered (V)	(I) > (III) > (V)
		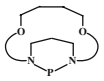 6-membered (IV)	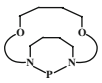 7-membered (VI)		(IV) > (VI)
		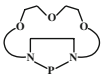 5-membered (4)	 6-membered (5)		(4) > (5)
X=Cl, Y= 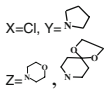	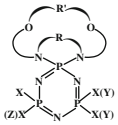	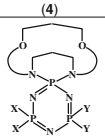 (VII)	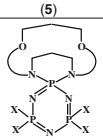 (III)		(VII) > (III)
		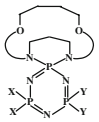 (VIII)	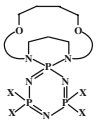 (IV)		(VIII) > (IV)
		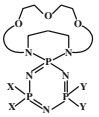 (9)	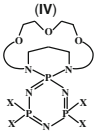 (5)		(9) > (5)
		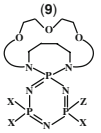 (13)	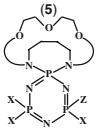 (14)		(13) > (14)

the types A and C in region A. The homologous compounds Fig. 9b can be comparable with each other. Based on the electron releasing capacity of the *spiro*-crypta group, it has been made an order in Table 7. Type D compounds (**IX** and **X**) are ditopic, while the others are monotopic. As expected, the electron releasing powers of two macrorings are greater than that of one macroring. In addition, when the number of atoms increase in the macroring, the electron releasing capacity of the macroring decreases. The electron releasing powers of macrorings are in the following order: macrorings with five membered crypta rings > macrorings with six membered crypta rings > macrorings with seven membered crypta rings. When we compared the geminal pyrrolidine substituted phosphazenes (type B) with the phosphazenes (type A), it is observed that the electron releasing power of pyrrolidino groups in **VII** and **VIII** are

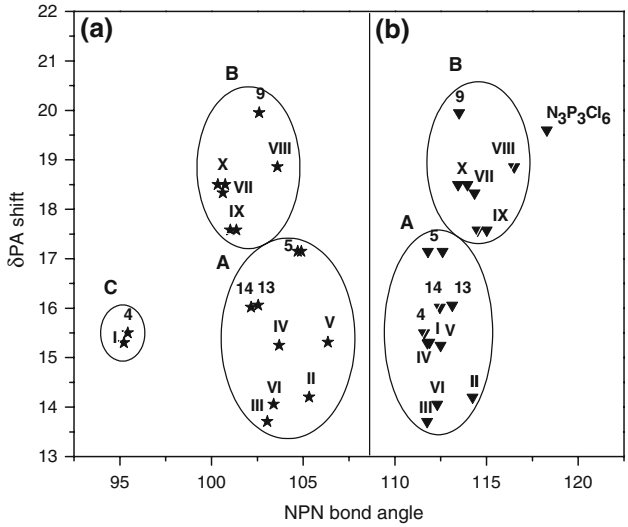

Fig. 8 The relationship between NPN bond angles and δP_A-shifts. $\delta(PCl_2)$ and the α-values of $N_3P_3Cl_6$ are 19.60 ppm and 118.30(2)° [37]

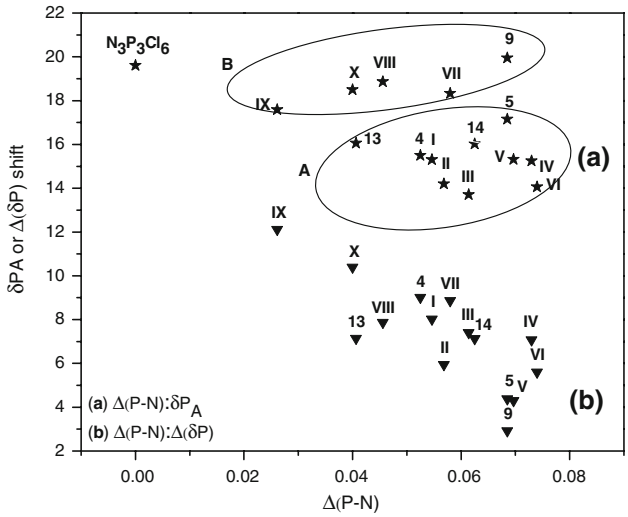

Fig. 9 The relationship between Δ(P–N) and Δ(δP) and δP_A-shifts

greater than those of the chloro groups in **III** and **IV**. Interestingly, Δ(P–N) values of **9** in type B and **5** in type A are the same. In case of mono substituted phosphazenes (type C), the electron releasing capacity of morpholino group is much larger than that of DASD.

Conclusions

In this study, the new substituted *spiro*-crypta phosphazene derivatives (**7**, **8**, **10**–**14**) have been obtained. According to the ^{31}P NMR spectra of fully substituted counterparts (**7**, **8** and **10**), these compounds have anisochrony. In addition, *spiro*-cyclic nitrogen atoms of **9** are stereogenic, as indicated by the X-ray crystallographic data. The variations of δP-shifts depend on the steric and electronic factors of bulky substituents, which change the angles of the phosphazene ring. The correlation of the endocyclic (α) and exocyclic (α′) NPN bond angles with δP_{spiro}-shifts has been investigated. Meanwhile, the relationships between Δ(P–N) versus the δP_{spiro}-shifts and Δ(δP) values have been presented. No linear relationship has been observed. The points appear as a "cluster" in Figs. 8 and 9.

Supplementary data

Crystallographic data for the structures reported here have been deposited at the CCDC as supplementary data, CCDC nos. 604056 for **9**, 716636 for **13** and 716637 for **14**. Copies of the data can be obtained on application to CCDC, 12 Union Road, Cambridge CB2 1EZ, UK. E-mail: deposit@ccdc.cam.ac.uk.

Acknowledgements The authors acknowledge The Scientific and Technical Research Council of Turkey (grant no. 104T392),and Hacettepe University, Scientific Research Unit (grant no. 02 02 602 002) for financial support.

References

1. Marck, J.E., Allcock, H.R., West, R.: Inorganic Polymers, 2nd edn. Oxford University Press, New York (2005)
2. Benson, M.A., Steiner, A.: Connecting cyclophosphazene via ring N-centers with covalent linkers. Chem. Commun. (Camb.). 5026–5028 (2005). doi:10.1039/b510898e
3. Mathew, D., Nair, C.P.R., Ninan, K.N.: Phosphazene–triazine cyclomatrix network polymers: some aspects of synthesis, thermaland flame-retardant characteristics. Polym. Int. **49**, 48–56 (2000). doi:10.1002/(SICI)1097-0126(200001)49:1<48::AID-PI309>3.0.CO;2-M
4. Zhang, Y., Huynh, K., Manners, I., Reed, C.A.: Ambient temperature ring-opening polymerization (ROP) of cyclic chlorophosphazene trimer($N_3P_3Cl_6$) catalyzed by silylium ions. Chem. Commun. (Camb.). 494–496 (2008). doi:10.1039/b713933k
5. Allcock, H.R., Napierala, M.E., Cameron, C.G., O'Connor, S.J.M.: Synthesis and characterization of ionically conducting alkoxy ether/alkoxy mixed-substituent poly(organophosphazenes) and their use as solid solvents for ionic conduction. Macromolecules **29**, 1951–1956 (1996). doi:10.1021/ma951391i
6. Xu, G., Lu, Q., Yu, B., Wen, L.: Inorganic polymer phosphazene disulfide as cathode material for rechargeable lithium batteries. Solid State Ion. **177**, 305–309 (2006). doi:10.1016/j.ssi.2005.10.029
7. Allcock, H.R., Wood, R.M.: Design and synthesis of ion-conductive polyphosphazenes for fuel cell applications: review. J. Polym. Sci. B Polym. Phys. **44**, 2358–2368 (2006). doi:10.1002/polb.20864
8. Greish, Y.E., Bender, J.D., Lakshmi, S., Brown, P.W., Allcock, H.R., Laurencin, C.T.: Low temperature formation of

hydroxyapatite-poly(alkyl oxybenzoate)phosphazene composites for biomedical applications. Biomaterials **26**, 1–9 (2005). doi:10.1016/j.biomaterials.2004.02.016

9. Singh, A., Krogman, N.R., Sethurman, S., Nair, L.S., Sturgeon, J.L., Brown, P.W., Laurencin, C.T., Allcock, H.R.: Effect of side group chemistry on the properties of biodegradable L-alanine cosubstituted polyphosphazenes. Biomacromolecules **7**, 914–918 (2006). doi:10.1021/bm050752r
10. Carriedo, G.A., Garcia-Alonso, J.F., Garcı'a-Alvarez, L.J., Pappalardo, G.C., Punzo, F., Rossi, P.: Stereoisomer discrimination through π-stacking interactions in spirocyclic phosphazenes bearing 2,2′-dioxybiphenyl units. Eur. J. Inorg. Chem. **2003**(13), 2413–2418 (2003)
11. Shimono, S., Takahashi, H., Sakai, N., Tamura, R., Ikuma, N., Yamauchi, J.: Use of cyclotriphosphazene as a molecular scaffold for building chiral multispin systems. Mol. Cryst. Liq. Cryst. **440**, 37–52 (2005). doi:10.1080/15421400590957657
12. Gleria, M., De Jaeger, R.: Aspects of phosphazene research. Inorg. Organomet. Polym. **11**, 1–45 (2005). doi:10.1023/A:1013276518701
13. Çaylak, N., Hökelek, T., Bilge, S., Özgüç, B., Kılıç, Z.: 4,4,6,6-Tetrachloro-2,2-(ethylenedioxydi-o-phenylenediimino)-2λ^5,4λ^5,6λ^5-cyclotriphosphazene. Acta Crystallogr. C **60**, 461–463 (2004). doi:10.1107/S0108270104010169
14. Tercan, B., Hökelek, T., Bilge, S., Özgüç, B., Kılıç, Z.: 4,4,6,6-Tetrachloro-2,2-(propylenedioxydi-o-phenylenediimino)-2λ^5,4λ^5,6λ^5-cyclotriphosphazene. Acta Crystallogr. C **60**, 381–383 (2004). doi:10.1107/S0108270104006894
15. Özgüç, B., Bilge, S., Çaylak, N., Demiriz, Ş., İşler, H., Havyalı, M., Kılıç, Z., Hökelek, T.: Phosphorus–nitrogen compounds: novel *spiro*-cyclophosphazenic lariat (PNP-pivot) ether derivatives. Structures of 4,4,6,6-tetrachloro-2,2-[3-oxa-1,5-pentane dioxy bis(2-phenyl-amino)]cyclo-2λ^5,4λ^5,6λ^5-triphosphazene and 4,4,6,6-tetrachloro-2,2-[1,2-xylylene dioxy bis(2-phenylamino)]cyclo-2λ^5,4λ^5,6λ^5-triphosphazene. J. Mol. Struct. **748**, 39–47 (2005). doi:10.1016/j.molstruc.2005.02.015
16. Asmafiliz, N.G.: Synthesis of crypta phosphazene derivatives. Master Dissertation, Ankara University, Ankara, Turkey (2005)
17. Bilge, S., Kılıç, Z., Çaylak, N., Hökelek, T.: Phosphorus–nitrogen compounds: novel spiro-crypta-phosphazenes. Structure of {pentane-3-oxa-NAN′-bis(1,5-ox benzyl)-spiro (propane-1′,3′-diamino)-4,4,6,6-tetrachlorocyclo-2λ^5,4λ^5,6λ^5-triphosphazatriene. J. Mol. Struct. **707**, 139–146 (2004). doi:10.1016/j.molstruc.2004.07.009
18. Tercan, B., Hökelek, T., Bilge, S., Demiriz, Ş., Kılıç, Z.: 4,4,6,6-Tetrachloro-1′,3′-[2,2′-(3-oxapentane-1,5-dioxy)dibenzyl]-2λ^5,4λ^5,6λ^5-cyclotriphosphazene-2-spiro-2′-1,3,2-diazaphospholanebenzene-hemisolvate. Acta Crystallogr. **E60**, 1369–1372 (2004)
19. Bilge, S., Demiriz, Ş., Okumuş, A., Kılıç, Z., Tercan, B., Hökelek, T., Büyükgüngör, O.: Phosphorus-nitrogen compounds: part 13. Syntheses, crystal structures, spectroscopic, stereogenic and anisochronic properties of novel *spiro-ansa-spiro-*, *spiro-bino-spiro-* and *spiro-*. Crypta phosphazene derivatives. Inorg. Chem. **45**, 8755–8767 (2006)
20. Asmafiliz, N., İlter, E.E., Işıklan, M., Kılıç, Z., Tercan, B., Çaylak, N., Hökelek, T., Büyükgüngör, O.: Novel phosphazene derivatives. Synthesis, anisochronism and structural investigations of mono- and ditopic spiro-crypta phosphazenes. J. Mol. Struct. **832**, 172–183 (2007). doi:10.1016/j.molstruc.2006.08.017
21. İlter, E.E., Çaylak, N., Işıklan, M., Asmafiliz, N., Kılıç, Z., Hökelek, T.: Phosphorus-nitrogen compounds. *spiro-* and Crypta-phosphazene derivatives: synthesis and spectral investigations. J. Mol. Struct. **697**, 119–129 (2004). doi:10.1016/j.molstruc.2004.03.043
22. Asmafiliz, N., İlter, E.E., Kılıç, Z., Hökelek, T., Şahin, E.: Synthesis, anisochronism and the relationship between crystallographic and spectral data of monotopic spiro-crypta phosphazenes. J. Chem. Sci. **120**(4), 363–376 (2008). doi:10.1007/s12039-008-0060-x
23. Tercan, B., Hökelek, T., Büyükgüngör, O., Asmafiliz, N., İlter, E.E., Kılıç, Z.: 7,11-[butane-1,4-diyldioxydi-o-phenylne-dimethylene-6,6-dichloro-4,4-bis(pyrrolidino)2λ^5, 4λ^5, 6λ^5-triphosphaza-1,3,5,7,11-pentaazaspiro [5.5]-undeca-1,3,5-triene. Acta Crystallogr. **E61**, 2145–2147 (2005)
24. Bilge, S., Natsagdorj, A., Demiriz, Ş., Çaylak, N., Kılıç, Z., Hökelek, T.: Phosphorus-nitrogen compounds: novel spirocyclic phosphazene derivatives. Structure of 3,3′-propane-1,3-diyl-bis[4′,4′,6′,6′-tetrachloro-3,4-dihydrospiro[1,3,2-benzoxazaphosphorine-2,2′λ^5-[4λ^5, 6λ^5][1,3,5,2,4,6]triazatriphosphorine]]. Helv. Chim. Acta **87**, 2088–2099 (2004). doi:10.1002/hlca.200490188
25. Safran, S., Hökelek, T., Bilge, S., Demiriz, Ş., Natsagdorj, A., Kılıç, Z.: Crystal structure of 8,8-dichloro-1,2,10,11,13,14-hexahydro-6λ^5,8λ^5,10λ^5-6,10-nitrilo[1,3,5,7,2,4,6] tetratriphos-phoninobis[1,3,2]oxaza phosphorine. Anal. Sci. **21**, 77–78 (2005). doi:10.2116/analsci.21.77
26. Tercan, B., Hökelek, T., Bilge, S., Natsagdorj, A., Demiriz, Ş., Kılıç, Z.: 6′,6′-Dichloro-3,3″-etheno-3,4,3″,4″-tetrahydro-2H-1,3-benzoxazine-2-spiro-2′)-(2λ^5,4λ^5,6λ^5 cyclotriphosphazene)-4′-spiro-2″-2H-1,3-benzoxazin. Acta Crystallogr. **E60**, 795–797 (2004)
27. Ilter, E.E., Asmafiliz, N., Işıklan, M., Kılıç, Z., Hökelek, T., Çaylak, N., Şahin, E.: Phosphorus-nitrogen compounds: part 14. Synthesis, stereogenism and structural ınvestigations of novel N/O spirocyclic phosphazene derivatives. Inorg. Chem. **46**(23), 9931–9944 (2007). doi:10.1021/ic701216f
28. Hökelek, T., Akduran, N., Yıldız, M., Dal, H., Kılıç, Z.: 2,4-[2,2′-Methylenebis(4-nitrophenoxy)]-2,4,6,6-tetra chloro cyclo-2λ^5,4λ^5,6λ^5-triphosphazatriene (ansa). Acta Crystallogr. C **56**, 90–92 (2000). doi:10.1107/S0108270199012986
29. Öztürk, L., Hökelek, T., Dal, H., Kılıç, Z.: 2,2-[2,200-Methylene-bis(4-nitrophenoxy)]-4,6-[2,2′-methylenebis(4-nitro phenoxy)]-4,6-dichloro-1,3,5,2λ^5,4λ^5,6λ^5-triazatriphosphorine (spiro-ansa) acetonitrile. Acta Crystallogr. **E58**, 20–23 (2001)
30. Perin, D.D., Armarego, W.L., Perrin, D.R.: Purification of Laboratory Chemicals, 2nd edn. Pergamon, Oxford (1980)
31. Hökelek, T., Akduran, N., Bilge, S., Kılıç, Z.: Crystal Structure of 3,4,6,7,15,16,17,18,19,20,21-Undecahydro-2,5,6-trioxa-16,20-diazatricyclo [20.4.0.0^{9,14}] hexacosa-9,11,13,22,24,26(1)-hexaene. Anal. Sci. **17**, 801–802 (2001). doi:10.2116/analsci.17.801
32. Hökelek, T., Bilge, S., Kılıç, Z.: 1,15-Diaza-3,4:12,13-dibenzo-5,8,11-trioxacycloheptadecane hemihydrate. Acta Crystallogr. **E59**, 1607–1609 (2003)
33. North, A.C.T., Phillips, D.C., Mathews, F.S.: A semi-empirical method of absorption correction. Acta Crystallogr. A **24**, 351–359 (1968). doi:10.1107/S0567739468000707
34. Bruker.: SADABS. Bruker AXS Inc., Madison, Wisconsin, USA (1996)
35. Sheldrick, G.M.: A short history of SHELX. Acta Crystallogr. A **64**, 112–122 (2008). doi:10.1107/S0108767307043930
36. Farrugia, L.J.: *ORTEP-3* for Windows—a version of *ORTEP-III* with a Graphical User Interface (GUI). J. Appl. Cryst. **30**, 565 (1997). doi:10.1107/S0021889897003117
37. Bullen, G.J.: Improved determination of the crystal structure of hexachlorocyclotriphosphazene. J. Chem. Soc. A 1450–1453 (1971). doi:10.1039/j19710001450
38. Goodwin, H.J., Henrick, K., Lindoy, L., McPartlin, M., Tasker, P.A.: Studies of macrocyclic ligand hole sizes. 1. X-ray structures of the nickel bromide complexes of the diimine and reduced forms

of a 16-membered macrocyclic ring incorporating O_2N_2 donors. Inorg. Chem. **21**, 3261–3264 (1982). doi:10.1021/ic00139a002

39. Bilge, S., Coles, S.J., Davies, D.B., Hursthouse, M.B., Kılıç, Z., Rutherford, J.S., Shaw, R.A.: The clathrate and channel inclusion systems co-exist in the crystal structure of a bis-C-pivot lariat ether. CrystEngComm **10**, 873–878 (2008). doi:10.1039/b716882a
40. Bilge, S., Özgüç, B., Safran, S., Demiriz, Ş., İşler, H., Hayvalı, M., Kılıç, Z., Hökelek, T.: Phosphorus–nitrogen compounds: novel fully substituted *spiro*-cyclophosphazenic lariat (PNP-pivot) ether derivatives. Structures of 4,4,6,6-tetrapyrrolidino-2,2-[3-oxa-1,5-pentane dioxy bis(2-phenylamino)]cyclo-2λ^5,4λ^5,6λ^5-triphosphazene and 4,4,6,6-tetrapyrrolidino-2,2-[1,2-xylylene dioxy bis(2-phenylamino)]cyclo-2λ^5,4λ^5,6λ^5-triphosphazene. J. Mol. Struct. **748**, 101–109 (2005). doi:10.1016/j.molstruc.2005.03.018
41. Beşli, S., Coles, S.J., Davies, D.B., Hursthouse, M., Kılıç, A., Mayer, T., Shaw, R.A.: Structural investigations of phosphorus-nitrogen compounds. 5. Relationships between molecular parameters of 2,2-diphenyl-4,6-cis-oxytetra (ethyleneoxy)-4,6-R2-cyclotriphosphazatrienes (R = Cl, OCH_2CF_3, OPh, OMe, NHPh, NHBut) and substituent basicity constants. Acta Crystallogr. B **58**, 1067–1073 (2002). doi:10.1107/S0108768102018608